Dissociation of Carbon Monoxide on the Rhenium(10-10) Surface†

C. Pauls, D. Przyrembel, and K. Christmann*

Institut für Chemie der Freien Universität, Bereich Physikalische und Theoretische Chemie, Takustr. 3, D-14195 Berlin, Germany

Received: March 31, 2004; In Final Form: July 16, 2004

We have studied the interaction of carbon monoxide with a Re(10-10) surface between 150 and 800 K by means of low-energy electron diffraction (LEED), temperature-programmed thermal desorption, and work function change ($\Delta\varphi$) measurements. We find two (temperature-dependent) interaction/reaction channels: At 200 K, CO forms molecular (α) states with binding energies between 95 and 118 kJ/mol. At a coverage of $\Theta_{CO} = 0.5$, a c(2 × 2) LEED phase forms; for $\Theta_{CO} > 0.5$, a dim (2 × 3) structure is observed. The work function change of $\Delta\varphi_{max} = +780$ meV indicates negatively polarized adsorbed CO molecules. Exposure at 500 K exclusively yields dissociated CO as deduced from high-temperature β desorption states (185 kJ/mol $< E_{des} <$ 210 kJ/mol), second-order reaction kinetics, and the formation of a sharp (1 × 2) LEED pattern at $\Theta_{CO} = 0.25$ ($\Theta_C + \Theta_O = 0.50$) associated with the least strongly bound β_1 CO state. $\Delta\varphi_{max}$ amounts to merely +400 meV. Smaller CO coverages ($0.125 < \Theta < 0.16$) give rise to a c(2 × 4) LEED structure. Upon heating, but prior to desorption, both superstructures undergo an order−disorder phase transition. Our results are discussed in terms of face specifities of CO dissociation, CO binding states, and structures and are compared with previous work on CO interaction/dissociation on related transition-metal surfaces.

1. Introduction

Although the interaction of carbon monoxide with transition-metal surfaces is believed to be well understood,[1−4] there still remain some open questions concerning, for example, the tendency of certain transition-metal surfaces to dissociatively adsorb CO, depending on their crystallographic orientation. Brodén et al.[5] reported already in 1976 on a trend whereafter the energy separation Δ between the 1π and 4σ molecular orbital levels of adsorbed CO increases leftwards along each row and upward in each column of the periodic table. In addition, the quantity Δ was considered an indicator of the bond strength between the C and the O atom in the adsorbed state. All metals that are able to dissociate CO lie to the left of the periodic table, with a borderline from bottom left to top right separating the active from inactive metals. While the authors regarded the influence of the surface geometry as a second-order effect only, they admitted such an influence for those metals that are positioned right at the borderline, i.e., Fe and Co, Tc and Ru, and W and Re. For example, the W(100) surface was found to be active[6,7] but the (more densely packed) (110) surface *inactive* for CO dissociation.[3,8] Later, theoretical calculations by Andreoni and Varma[9] confirmed the trends reported by Brodén et al., whereafter the position of the metal substrate in the periodic table (and, hence, its electronic structure) is crucial. The CO interaction with transition-metal surfaces is usually described by the Blyholder donor−acceptor model.[10] In this model, a strong CO−metal bond is favored by a high density of d electron states near the Fermi level. Recent theoretical calculations by Mavriakakis et al.[11] for CO interaction with strained metals came to the conclusion that, for a given metal, the center of gravity of the d electronic states depends strongly on the coordination of the surface atoms. A reduced coordination (verified for the "open" hexagonal close packed (hcp) (10-10) surface) will shift the center of gravity of the d electrons closer to E_F and, hence, support the formation of a strong CO−metal donor−acceptor complex. Consequently, dissociation of the C−O bond can more easily occur.

In our work on the CO interaction with Re surfaces, we came across a clear influence of this surface geometric effect in that the flat and smooth Re(0001) surface[12] did practically not dissociate CO, while the crystallographically more open (10-10) orientation was extremely active in that respect. CO adsorption on Re has been studied quite extensively, in particular for the (0001) surface by Ducros et al.,[13−17] Braun et al.,[18,19] and He and Goodman.[20] Less studies are available concerning CO interaction with the (10-10) surface, namely, an early low-energy electron diffraction (LEED) report[21] and a study of the coadsorption between sulfur and CO.[22] However, the CO dissociation activity was practically not addressed. As we will show, just this surface readily dissociates CO, the products C and O forming characteristic LEED superstructures. A most widely used experimental tool to study adsorption phenomena is temperature-programmed thermal desorption (TPD).[24] On all Re surfaces investigated so far, TPD shows two sets of CO desorption peaks reflecting the molecular α states in the low-temperature range and the dissociated β states between 600 and 1000 K, in agreement with observations on other CO/metal adsorption systems.[25] At least for Re(0001), Ducros et al.[16] have proven the dissociated nature of the β states via X-ray photoelectron spectroscopy and vibrational loss spectroscopy (HREELS), although the fraction of dissociated CO merely amounts to ca. 10%.[13] Systematic studies using stepped Re-(0001) surfaces revealed that the CO dissociation occurs preferentially at step and defect sites.[15,16] The undefined defect concentration of their Re(0001) surfaces is probably the reason the results of Ducros et al.[13−16] differ from the ones by He and

† Part of the special issue "Gerhard Ertl Festschrift".

* To whom correspondence should be addressed. E-mail: kchr@chemie.fu-berlin.de.

10.1021/jp040271m CCC: $27.50
Published on Web 08/04/2004

Goodman.[20] In a recent catalytic study, we could show that small amounts of gold deposited onto Re(0001) entirely suppress Re's activity to dissociate CO. It is believed that the Au atoms decorate the Re step sites and deactivate them for CO dissociation.[12] The formation of the (dissociated) β states is thermally activated. Molecularly adsorbed CO undergoes dissociation into C and O species beyond 380 K;[17] further heating makes the dissociated fragments recombine to CO, which then leaves the surface as β state(s). If this recombination process is rate limiting, second-order desorption kinetics results. This kinetics exactly was found for CO β-state desorption from a W(100) surface, underlining the recombination reaction between CO's dissociation fragments.[23] Quite surprisingly, a second-order has never been observed for the β-CO desorption from Re(0001). Rather, the kinetics is of first order, which could indicate that the C and O atoms remain in close proximity after the dissociation. Concerning the Re(10-10) orientation, the scarce CO TPD data published so far[22] did not allow a determination of the respective desorption kinetics. Here, we report the results of a combined LEED, TPD, and $\Delta\varphi$ investigation into the CO interaction with a chemically clean, well-defined Re(10-10) substrate spanning the temperature range from 200 to 800 K.

2. Experimental Section

The measurements were performed in an ultrahigh vacuum (UHV) system equipped with standard spectroscopic tools (4-grid reverse-view LEED, retarding-field Auger electron spectroscopy (AES), quadrupole mass spectrometer, homemade Kelvin probe) and a combined turbomolecular and titanium sputter pumping system. Research-grade CO gas (3,7 Linde) was taken from a "Minican" gas cylinder and admitted to the UHV system via a bakeable leak valve. Considering all uncertainties of the pressure readings, our absolute pressure values are uncertain to within 25%. However, the *relative* pressure (and exposure) values are much more accurate. The ultrapure Re crystal (5N, MaTech) was X-ray oriented to the (10-10) direction, cut and polished to within 0.2°, and mounted on the manipulator with resistive ($T_{max} = 1600$ K) and electron bombardment ($T_{max} = 2300$ K) heating facilities. Temperature was controlled with a Re/WRe thermocouple; extremely linear heating ramps were obtained by a programmable power supply (TET electronics) and appropriate computer software. A liquid N_2 reservoir also allowed cooling of the sample to ~150 K. Sample cleaning was achieved by repeated cycles of gentle O_2/H_2 oxidation/reduction cycles and subsequent high-temperature flashing and annealing[26,27] and controlled by AES, $\Delta\varphi$, and LEED, cf. Figure 1a. Concerning the crystallography of the Re-(10-10) surface, we refer to previous LEED structure analyses: [28,29] The relatively "open" surface consists of alternating Re rows and troughs parallel to the [1-210] direction and is terminated by the "less-corrugated double termination" A.[28] Previous and recent LEED structure analyses[28,29] revealed that the surface is inward relaxed but not reconstructed. Concerning the CO coverage calibration, we use the common definition in which $\Theta = 1$ refers to the number of topmost surface atoms, i.e., equals 8.13×10^{18} atoms or molecules/m^2. We understand the (hypothetical) CO coverage $\Theta_{CO} = 1$ as if every Re row atom nominally carries one adsorbed CO molecule.

To obtain background-free TD spectra, we used a quadrupole mass spectrometer mounted inside a separately differentially pumped cone. The line-of-sight contact with the sample was achieved only by a 4 mm diameter orifice, which accepted the desorbing molecules at a distance of less than 0.5 mm to the sample surface. Linearity of the heating rate (commonly used

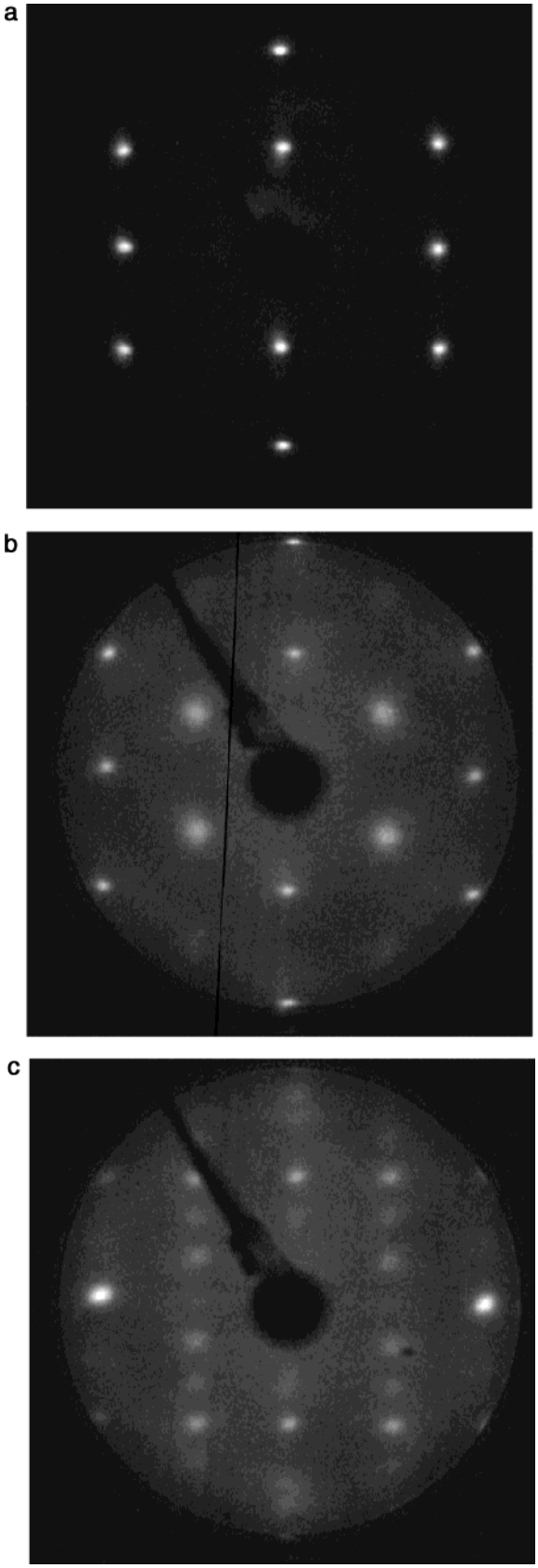

Figure 1. LEED patterns of the CO/Re(10-10) system at $T = 200$ K: (a) (1 × 1) pattern of the clean surface (electron energy $E_p = 76$ eV); (b) c(2 × 2) pattern induced by half a monolayer of adsorbed CO ($\Theta_{CO} = 0.5$), ($E_p = 57$ eV); (c) (2 × 3) pattern after gentle annealing at ambient CO pressure of 2×10^{-8} mbar ($E_p = 52$ eV).

dT/dt = 4.8 K/s); temperature measurement and amu data acquisition were computer-controlled. The TPD spectra were

analyzed according to the Redhead method[31] and the direct application of the Polanyi−Wigner equation,[32] cf. section 3.2. The $\Delta\varphi$ measurements were performed with a Kelvin-probe setup operating in a self-compensating manner using a PAR 124-Lock-In amplifier; the signal could be measured with an accuracy of about 2 meV.

3. Results

3.1. LEED. Our LEED experiments were performed at two different conditions. (i) The sample was kept at 200 K during exposure, and (ii) CO was adsorbed at $T = 500$ K, see below.

(i) At 200 K, CO adsorbs practically entirely as intact molecules; the dissociation channel does not yet play a role. Without annealing, we could not distinguish any CO "extra" LEED spots but quite a diffuse intensity distribution with large clouds or globules in certain areas of k space. Apparently, the adsorbed molecules are far too immobile to form a phase with sufficient long-range order. Gentle annealing around 250−300 K generated a relatively sharp c(2 × 2) pattern, especially if we had exposed as much CO as was necessary to fill the α_3 TPD state (∼3 L). An ambient CO dosing pressure of 2×10^{-8} mbar and gentle heating was necessary to obtain a dim p(2 × 3) LEED pattern, however, with considerable remanent disorder, indicating a final molecular CO phase at a coverage between 0.5 and 0.7. Heating of these molecular phases to about 350 K produced additional spots of a p(1 × 2) LEED pattern which gained intensity during heating, while at the same time the "molecular" spots disappeared, the reason being the increasingly competing CO dissociation. The whole sequence of LEED patterns due to adsorbed CO *molecules* is reproduced as Figure 1, including the LEED pattern of the clean Re(10-10) surface for comparison. We emphasize that we never succeeded in obtaining a (2 × 1)p2mg LEED phase.

(ii) CO was exposed to the Re sample kept at 500 K, for reasons explained below. Only then a c(2 × 4) superstructure appears after an exposure of 0.5 L. Around 0.75 L, the characteristic "extra" spots (*n*/2, *m*/4) become weaker, while a p(1 × 2) structure slowly develops which reaches maximum (and then exposure-independent) intensity after ∼3 L CO exposure. The two respective LEED patterns are shown in Figure 2. The p(1 × 2) phase has already been observed by Zehner and Farnsworth,[21] but not the c(2 × 4). Upon heating of the fully developed p(1 × 2) phase, the LEED pattern relatively sharply (temperature interval $\Delta T = 15$ K) disappears. If the heating is stopped immediately after the disappearance of the p(1 × 2) intensity around 660 K and the sample is allowed to cool, the fractional-order "extra" spots of the p(1 × 2) reappear without any loss of intensity. Apparently, the p(1 × 2) phase undergoes an order−disorder phase transition with a critical temperature $T_{C,1\times2}$ lying somewhere between 650 and 660 K. However, extended heating to beyond 660 K removes CO (see section 3.2) and makes the p(1 × 2) phase irreversibly disappear. Similar to the p(1 × 2), the c(2 × 4) phase undergoes an order−disorder transition upon heating; it can never be observed for $T > 650$ K. However, if we desorb an appropriate amount of CO out of the p(1 × 2) phase and lower the temperature to below 600 K, the c(2 × 4) phase reappears.

The exposure and coverage dependences of the two ordered phases (c(2 × 4) and p(1 × 2)) at 500 K are summarized in Figure 3. Also illustrated is the Θ-dependent desorption energy $E_{des}(\Theta)$ obtained from a TPD analysis, cf. section 3.2. There seems to be a close correlation between $E_{des}(\Theta)$ and the existence of the ordered phases, and we will take up this point in the Discussion. The LEED intensity vs Θ relation deserves interest, since there is not a sharp intensity maximum of the c(2 × 4)-related spots at the expected value of $\Theta = {}^1/_8$ but only a broad (plateaulike) maximum between $\Theta = 0.125$ and 0.17, while the p(1 × 2) intensity is steadily rising in this Θ range.

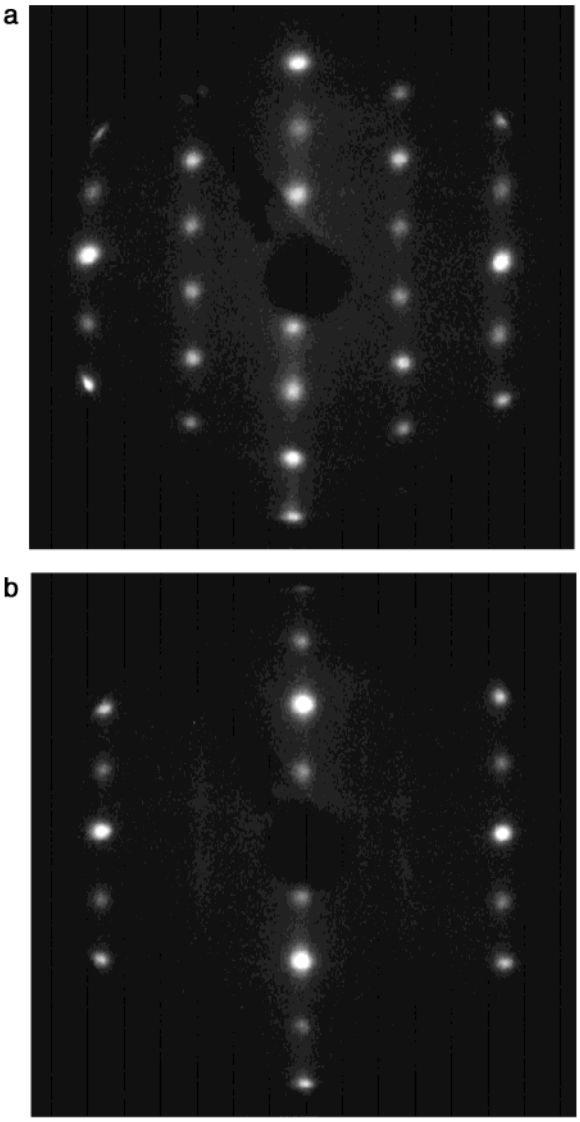

Figure 2. LEED patterns of the CO/Re(10-10) system at $T = 500$ K: (a) c(2 × 4) pattern at $\Theta_{CO} = 0.125$ ($T = 200$ K, $E_p = 53$ eV); (b) p(1 × 2) pattern at $\Theta_{CO} = 0.25$ ($T = 200$ K, $E_p = 54$ eV).

3.2. Thermal Desorption Spectroscopy. The rate of a thermal desorption reaction is usually described by the Polanyi−Wigner equation

$$R_{des} = -\frac{d\Theta}{dt} = \nu(\Theta,T)\Theta^x \exp\left(-\frac{\Delta E_{des}(\Theta,T)}{kT}\right) \qquad (1)$$

where ν is the frequency factor, x is the reaction order, and ΔE_{des} is the desorption energy.

Hence, TPD spectra can provide detailed information on the desorption energetics (exponent in eq 1), as well as on the kinetics (pre-exponential(s), reaction order(s), and coverage dependences). Moreover, the peak integrals $\int R_{des}\, dt$ are at least a relative measure of the amount of adsorbate present on the surface prior to the application of the temperature program. By comparing the actual adsorbed amount with the exposure, information about the (relative) sticking probability s and its coverage dependence is available.

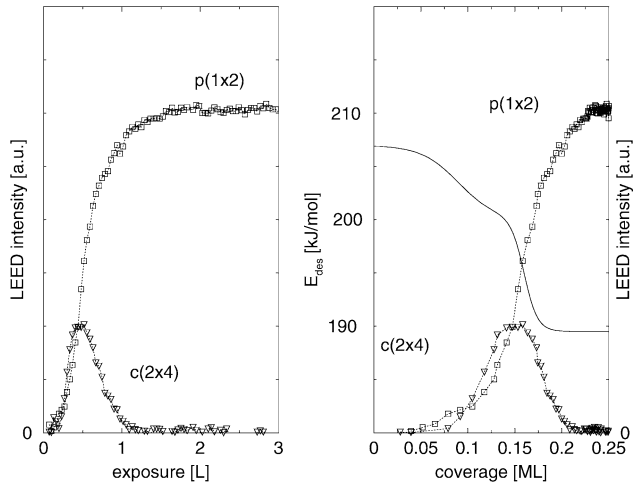

Figure 3. Exposure and coverage dependence of the LEED intensity of the (c(2 × 4) and p(1 × 2) phases at 500 K. Exposure dependence, left-hand frame; coverage dependence, right-hand frame. Included in the coverage dependence is the heat of CO desorption; transformation of the c(2 × 4) phase to the p(1 × 2) apparently costs ∼10 kJ/mol energy.

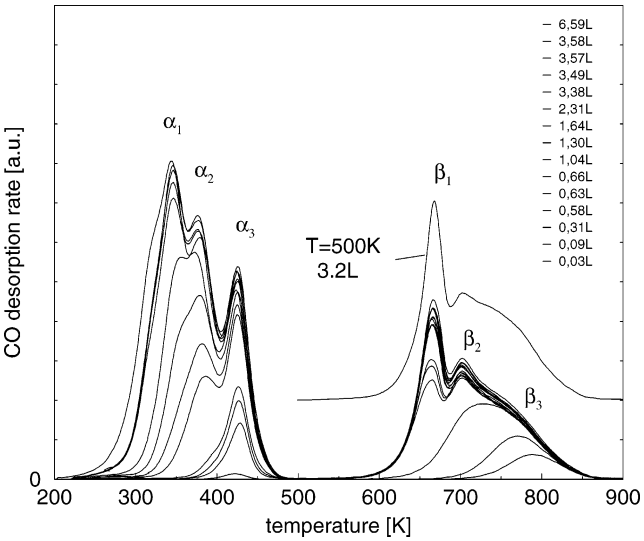

Figure 4. Series of CO thermal desorption spectra, taken with a heating rate of $\beta = 4.8$ K/s after adsorption at 200 K, for increasing CO exposures (Langmuir) at 200 K. The molecular α and the atomic β states are labeled; see text for further details.

3.2.1. The Energetics of Desorption. Again, we performed the CO exposure under *low-temperature* (200 K) and *high-temperature* conditions (500 K).

Exposure at 200 K led to TPD spectra shown in Figure 4. We follow the conventional notation (α states = molecularly adsorbed CO, β states = high-temperature, fragmented CO). Apart from some minor (although not unimportant) features, our spectra agree quite well with previous TD data published by Kelly et al.[22] We find three clear α states with increasing CO exposure. Their peak positions are practically invariant with CO exposure: α_3 appears at 430 K, α_2 at 380 K, and α_1 around 350 K. However, to completely restore the clean Re surface, we had to heat the sample to beyond 900 K and then find three more CO TD states, viz., the β_3 state desorbing, depending on the exposure, between 800 K (0.02 L) and ∼740 K (0.3 L), β_2 at 700 K, and the β_1 state at 665 K, β_1 and β_2 being almost invariant with CO exposure. A fourth (high-temperature) β state seen by Kelly et al.[22] could not be reproduced in our measurements. Another discrepancy with respect to Kelly et al.'s spectra

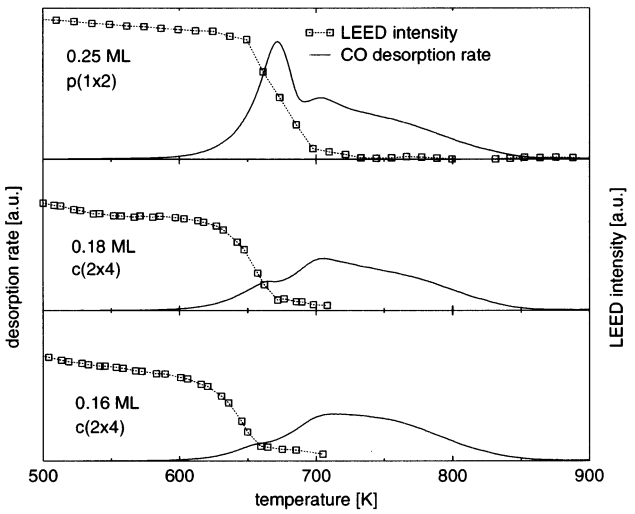

Figure 5. Decrease of the LEED intensities of the p(1 × 2) (upper curve) and the c(2 × 4) phase (lower curves) during CO desorption, for initial CO coverages of $\Theta_{CO} = 0.25$, 0.174, and 0.16, respectively. Also included are, for comparison, the corresponding thermal desorption spectra. The disappearance of the LEED structures is correlated with the respective CO β desorption states.

concerns the intensity ratios of the various states and their saturation exposures: They differ substantially in a sense that our saturation exposures are much smaller and our β_1 state is considerably more intense and sharper than the other β states.

By comparison of the thermal desorption spectra with the temperature dependence of the "extra" spot-LEED intensity (shown in Figure 5, upper curve), we can clearly associate the disappearance of the sharp β_1 state with the loss of p(1 × 2) intensity. Obviously, the p(1 × 2) long-range order is correlated with the CO β_1 binding state. In the same manner, we tried to determine the TPD state(s) responsible for the c(2 × 4) phase (Figure 5, middle and bottom curves). The problem is again that the c(2 × 4) intensity vanishes not because of the loss of CO but due to an order−disorder phase transition. Despite this difficulty to precisely associate a certain TPD spectrum with the c(2 × 4) phase, we got the impression that its formation is correlated with the filled β_2 and the beginning β_1 state. Interestingly, the most strongly held β_3 state is *not* associated with a long-range ordered phase.

The TPD series of Figure 4 suggests that no CO species leaves the surface between 480 and 580 K, thus allowing us to separate the β from the α desorption contributions simply by exposing the surface to CO at 500 K. By comparison of the 200-K (see above) with the 500-K TPD spectra, we found practically identical β desorption behavior, which means that the slow heating of a CO-covered surface beginning at 200 K and the direct CO exposure of the hot crystal do not lead to different dissociation paths.

Turning to the determination of the CO desorption energies from the TPD data, we applied, in the first instance, Redhead's analysis[31] and assumed thereby a constant pre-exponential factor $\nu = 10^{13}$/s. We obtained for the molecular α states the following values for E_{des}: $\alpha_1 = 95$ kJ/mol; $\alpha_2 = 103$ kJ/mol; $\alpha_3 = 118$ kJ/mol. For the β states, the analysis reveals: $\beta_1 = 185$ kJ/mol; $\beta_2 = 196$ kJ/mol; β_3 (evaluated according to Habenschaden-Küppers[33]) = 207 kJ/mol. The value of the most strongly bound molecular CO, viz., 118 kJ/mol, compares well with CO desorption energies on other surfaces and may therefore be taken as a reliable quantity for the initial binding energy of molecular CO on the Re(10-10) surface. For the same state, Kelly et al. arrived at a comparable value of 105 kJ/mol.[22]

Regarding the energetics of the β states, the fairly large activation energies for desorption reflect the demanding energetics of O and/or C reaction, note that in order to form a CO molecule from chemisorbed carbon and oxygen both the Re−C and the Re−O bond have to be cleaved and the respective orbital(s) rehybridized to make the C≡O bond. Our energies ranging between 185 and 220 kJ/mol are likewise entirely in line with those previously reported by Kelly et al. (β_1 = 175 kJ/mol, β_2 = 196 kJ/mol, and β_3 = 217 kJ/mol). Possible reasons for the formation of the variety of CO states will be discussed in section 4.

3.2.2. The Kinetics Of Desorption. The observed apparent first-order kinetics of all *molecular* α states is to be expected for associative adsorption and desorption of CO. More revealing, however, is the pronounced peak shift of the β_3 state, which suggests a second-order desorption kinetics. To determine the kinetic exponent *x*, we have taken the logarithm of eq 1 and plotted $\ln(-d\Theta/dt) - x \ln \Theta$ vs the reciprocal temperature. Provided ΔE_{des} is Θ independent in the coverage interval considered the correct choice of *x* should yield a straight line, whose (negative) slope reflects the desorption energy ΔE_{des}. From this plot, we obtain a clear second-order kinetics up to a coverage of ∼40% of the β states, which sheds light on the rate-limiting step of the respective desorption reaction. Prior to desorption, individual carbon and oxygen atoms have to recombine to a $[C\cdots O]^{\ddagger}$ transition complex, the precursor of the desorbing CO molecule. The second-order behavior at not too large coverages is a first piece of clear evidence of *dissociative* adsorption, and we will return to it in section 4. The complicated shape of the β desorption curves at higher coverages, however, suggests fairly complex desorption mechanism(s).

There is another obvious feature of the TPD spectra, namely, the common leading edge of the sharp β_1 state, which develops beyond 0.5 L exposure at 500 K and reflects a Θ-independent rate of desorption. While this edge is not prominent at small β_1 concentrations, it clearly appears with the *well-developed* β_1 state. According to eq 1, a Θ-independent desorption rate is equivalent to *zero-order desorption kinetics*. The evaluation yields an activation energy of 188 kJ/mol for the respective desorption reaction, which compares very well with the 185 kJ/mol of the Redhead analysis. The origin of this zero-order kinetics will be discussed in section 4.

In both series (200 and 500 K), saturation of the β states is practically obtained after 3−4 L CO exposure. The overall exposure dependence points to a fairly large CO sticking probability on Re(10-10) and is reproduced as Figure 6a, left diagram (top curve, T_{ads} = 200 K; bottom curve (containing only the β states), T_{ads} = 500 K). The slope of these curves reflects the coverage dependence of the sticking probability, $s(\Theta)$. For the 500-K data, we have plotted the *relative* sticking probability s/s_0 as a function of the *relative* coverage Θ/Θ_{max} in Figure 7. The data points can well be reproduced by a second-order Kisliuk model, modified by King and Wells[34] according to the expression

$$\frac{s}{s_0} = \frac{1}{1 + K\left(\frac{1}{\Theta_{00}} - 1\right)} \qquad (2)$$

with $\Theta_{00} = 1 - \Theta - 2\Theta(1-\Theta)/1 + ((1-4\Theta(1-\Theta)B))^{1/2}$ = probability for the occurrence of pairs of empty sites and the constant B containing the pairwise lateral interaction energies. The parameter K describes the lifetime of the precursor state.

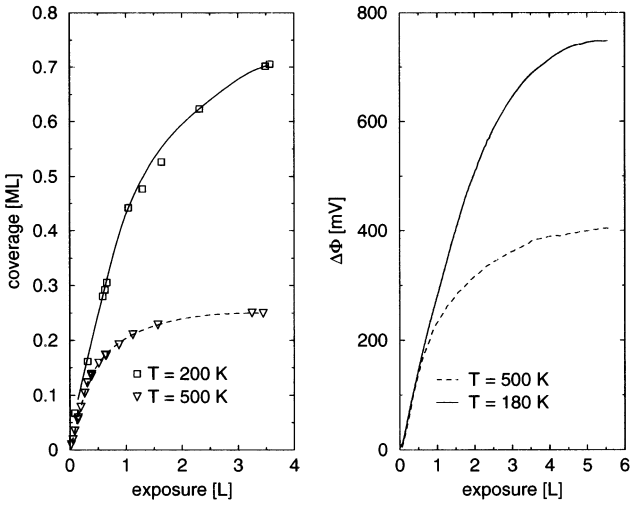

Figure 6. Exposure dependence of the CO coverage for 200 K (full lines) and 500 K (broken lines) as reflected by (a) the TPD uptake (determined by integration of the TPD spectra) and (b) the CO-induced change of the work function $\Delta\varphi$.

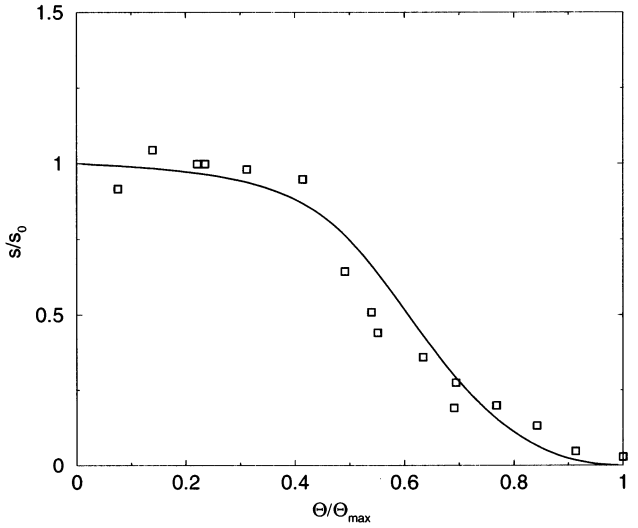

Figure 7. Dependence of the relative sticking coefficient s/s_0 on the relative C + O coverage, for CO adsorption on Re(10-10) at 500 K. The squares represent the data points; the solid line is the functional dependence of eq 2. The best-fit parameters are: $B = 0.915$; $K = 0.043$.

The obtained curve shape is characteristic of an adsorption into a well-ordered chemisorbed layer which is nicely compatible with our conclusions from LEED. Taking into account absolute CO coverages, we arrive at s_0 = 0.96 (±10%) for the 200-K series and s_0 = 0.84 (±10%) for the 500-K series. At 200 K, the saturation coverage is 0.71 and reached after ca. 4 L, while upon 500 K, CO exposure the much smaller saturation coverage of $\Theta^{sat} \approx 0.25$ is obtained already after 2.5 L. This temperature dependent sticking behavior is absolutely mirrored in the exposure dependence of the work function change, cf., Figure 6b and section 3.3.1.

3.2.3. The Absolute CO Coverage. The sum of C + O coverage associated with the p(1 × 2) phase (which, according to its lattice symmetry, *must* imply half a monolayer (or a multiple) of adsorbed particles) is Θ = 0.5. For stoichiometric reasons, this is a quarter of a monolayer of C and O atoms, respectively. In other words, only *a quarter of a monolayer* of (initially undissociated) CO molecules is responsible for the fully developed p(1 × 2) structure. (In principle, of course, the p(1 × 2) phase could also reflect 0.5 ML of *molecularly* adsorbed

CO. However, this assumption (apart from the fact that it could hardly explain the second-order desorption kinetics) leads to unphysical sticking coefficients close to 2.) We then arrive at a saturation coverage of $\Theta_{CO} = 0.71$, which is surprisingly small in terms of the number of available adsorption sites of the large and "open" (10-10) surface and in view of the saturation coverages reported for similarly structured (10-10) surfaces. It appears, however, quite reasonable if we consider the competing dissociation channel, cf. section 4, and the site blocking effect induced by the CO fragments which will definitely reduce the CO saturation coverage.

3.3. Work Function Change ($\Delta\varphi$) Measurements. Again, we distinguish work function measurements taken at ~200 K and at 500 K, for the reasons mentioned above.

3.3.1. *Adsorption* Effects. Figure 6b (full line) displays the variation of the CO-induced work function change ("$\Delta\varphi$") upon exposure *at 180 K*. As usual for CO chemisorption, we observe an initially linear increase of ca. +200 meV up to ~1 L then a slight change of slope to another linear section ranging up to ca. 500 meV after 2 L, until the curve gradually levels off and reaches saturation around 780 meV after ~5 L exposure.

In our $\Delta\varphi$ measurements at 180 K, two cases may be probed: (i) CO does *not* dissociate, all observed $\Delta\varphi$ features simply reflect the electric properties of the molecular CO species with their individual dipole moments. This would only be true if the CO dissociation requires a substantial activation energy, which most of the molecules do not possess at the fairly low adsorption temperature of 180 K. (ii) CO dissociation occurs (at least partially) already at 200 K, because the respective activation barrier is not large. Then the overall $\Delta\varphi$ is composed (in a nonresolvable way) of *both* molecular and atomic contributions. In case i, the individual dipole contributions are likewise superimposed, since the respective states are not filled strictly sequentially, but according to Boltzmann's statistics in a more or less *parallel* fashion.

For comparison, the CO-induced $\Delta\varphi$ at *500 K* exposure is shown in the dotted line of Figure 6b. There seems to be no deviation from linearity in the very small exposure region; the curve rather smoothly bends horizontally and finally reaches saturation after 5−6 L exposure at the considerably smaller $\Delta\varphi$ value of 400 meV. Since we know that all molecular CO is gone at 500 K, the total change of 400 meV must stem alone from the combined dissociated species C + O. Subtracting this $\Delta\varphi$ value from the one measured at 180 K yields 380 meV which may be attributed to the presence of the sum of the three molecular α species.

3.3.2. Desorption Effects. This is particularly evident from experiments in which the work function is followed during desorption as a function of temperature, i.e., $\Delta\varphi(T)$. Figure 8 illustrates this "$\Delta\varphi$ desorption" after CO saturation at 180 K, starting at the saturation value of 780 meV. We applied a linear temperature ramp (heating rate = 4.8 K/s) and followed the decrease of $\Delta\varphi$ as CO desorbs. For not too high heating rates, separation of the molecular α CO states from the β states is possible, because these states desorb in different temperature ranges. By electronic differentiation, we can even obtain a $d\Delta\varphi/dT(T)$ curve (broken line) that resembles our TPD spectra in many respects and renders a distinction between the individual states possible: A representative TPD trace is included in Figure 8 as a dotted line for comparison. The α contribution reduces the work function by ca. 380 meV, i.e., from 780 to ca. 400 meV, underlining the negative dipole moment of this species. The most strongly bound CO α_3 state contributes most to $\Delta\varphi$, the α_2 state much less, and the α_1 state practically nothing. After a small $\Delta\varphi$ plateau around 400 meV between 450 and 550 K, where neither desorption nor any other surface process takes place, the β desorption sets in, whereby one slight break in the s-shaped descending curve distinguishes the β_1 from the β_2 states, each of which contributes about 200 meV to the total work function change. The *decrease* of $\Delta\varphi$ thereby indicates that also the adsorbed C and O atoms carry a negative dipole moment.

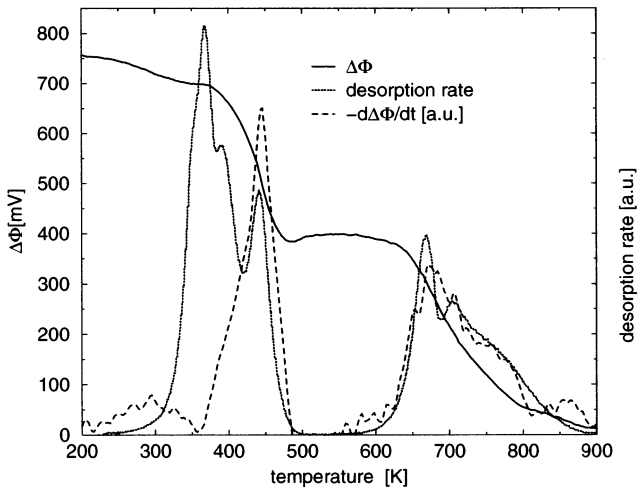

Figure 8. Temperature dependence of the CO-induced work function change ("$\Delta\varphi$ desorption"). The full line displays how $\Delta\varphi$ decreases with increasing temperature T (heating rate 4.8 K/s), thereby allowing a clear distinction between molecular and atomic desorption. Even more revealing is the derivation with respect to T, $d\Delta\varphi/dt$ (T) (broken line), which closely resembles the ordinary TPD spectrum (dotted line) except that $\Delta\varphi$ is "blind" for the molecular α_1 and α_2 states.

4. Discussion

4.1. Molecularly Adsorbed CO. Turning to the details of CO interaction with Re(10-10) and within this section to the *low-temperature adsorption* (200 K) first (which is dominated by molecular adsorption), we recall that up to four different molecular CO states can be distinguished in our TPD spectra. In principle, the multiplicity of these states can have a 2-fold origin: (i) the open geometry of the (10-10) orientation a priori provides various types of CO adsorption sites with potential wells of different depth or (ii) the diversity of these geometrically different sites is initially not pronounced, but the increasing CO coverage induces an *energetic heterogeneity* of the respective sites. Here, we may further distinguish two subcases: (a) the adsorbed CO molecules mutually interact and form various phases with long-range order. This is true for the hcp congeners Co(10-10)[35−37] and Ru(10-10)[38] as well as for the (geometrically similar) fcc(110) surfaces of Ni,[39,40] Rh,[41] Pd,[43,43] Pt,[44] and Ir(110),[45] on which CO dissociation does not occur. Yet, at least two or three CO TPD states are the rule. The second subcase (b) implies the formation of carbon and oxygen atoms due to CO dissociation. The respective fragments are usually strongly adsorbed and can greatly modify the surface electronic and adsorptive properties; in other words, a site diversity is produced a posteriori, and likewise complicated TPD spectra arise.

Various of the above cited papers, e.g., ref 43, aim at a correlation between the kind and number of ordered CO phases and the state multiplicity of the TD spectra, underlining that mutual CO−CO interactions are responsible for the phase formation and the TPD features. Applying this to our system CO/Re(10-10), we note that at least two molecular LEED phases

c(2 × 2) and (2 × 3) are formed but are instable already at 300 K and gradually convert to structures associated with CO fragments (c(2 × 4) and p(1 × 2)), especially under the electron beam, cf., section 4.2.

It is tempting to associate the fully developed low-temperature c(2 × 2) phase with a CO coverage of half a monolayer ($\Theta_{CO} = 0.5$) and with the first α_3 (and the second α_2) CO binding state, whereby the exact location of the CO molecule within the unit mesh is reserved to a future structural analysis. (This holds also for the high-coverage p(2 × 3) phase, which seems to be the final CO phase with long-range order). From HREELS data reported by Ducros et al.[16] for Re(0001)/CO and the published value for the CO stretching vibration, viz., 1990−2050 cm^{-1}, CO on Re seems to prefer a terminal (atop) coordination, similar to CO on Ru. Parallel to the formation of these ordered phases, however, the CO undergoes dissociation and self-inhibition of its adsorption due to the rising concentration of the dissociation products C and O, cf. section 4.2. Unfortunately, we cannot yet address the question as to what extent CO undergoes dissociation already at 200 K. The only nondestructive technique employed in our work, the $\Delta\varphi$ measurements, is not really helpful to delineate the molecular and the atomic CO species because of their very similar dipole moments. However, photoemission and vibrational loss measurements are in progress to tackle this problem.

The Re(10-10) surface so far is the only TM surface of 2-fold symmetry on which a coverage of $\Theta_{CO} = 1.0$ and the formation of a (2 × 1)p2mg phase[46] cannot be obtained, although the dimensions of the unit mesh would in principle allow the accommodation of two CO molecules in a single unit cell. The (2 × 1)p2mg phase with its glide-symmetry plane (reflecting a zigzaglike array of compressed CO molecules) has been reported for CO on the (10-10) and (110) surfaces, respectively, of Co, Ni, Ru, Rh, Pd, and Ir, and reflects the circumstance that an adsorbed CO occupies a circular area of almost 3-Å diameter.[47,48] The inevitable formation of C and O atoms on Re(10-10) caused by dissociation blocks sites for strong molecular CO adsorption and limits the saturation coverage to $\Theta_{CO,sat} = 0.71$, which is a much smaller value than that reported, for example, for the otherwise very similar Ru(10-10) surface with its $\Theta_{CO,sat} = 1.22$.[38] Of course, Ru(10-10) does *not* dissociate CO.

The detailed consideration of Re(10-10)'s activity for CO dissociation, cf. section 4.2, and our LEED observations reported in section 3.1 make us believe that the TPD state multiplicity stems from both the inherent crystallography of the (10-10) surface *and* the induced site heterogeneity due to C and O fragment atoms. Whether the "open" geometry *alone* could lead to the same multiplicity of the molecular CO binding states is difficult to answer, because heating is necessary to monitor TPD spectra and dissociation is then instantaneously induced.

The desorption energies found for the molecular states, especially the α_3 state with its ∼120 kJ/mol, lie within the expected range for CO interaction with hcp TM surfaces, although somewhere on the lower limit: For Co(10-10), Papp reported 145 kJ/mol,[36] for Ru(10−10), Lauth et al. found 150 kJ/mol,[38] while on Pd(110), Conrad et al.[49] measured an upper-limit value of 167 kJ/mol. For Rh(110), 133 kJ/mol[41] were communicated, while for Ni(110), Helms and Madix obtained 138 kJ/mol.[50] Also, the slight decrease with coverage evident from Figure 3 is typical for CO adsorption. One might also consider the face specifity of the Re−CO adsorptive bonding: A comparison of the molecular CO states of the (10-10) plane with those of the basal (0001) plane reveals, within the limits of accuracy, identical 120 kJ/mol for the most strongly bound α states,[12] pointing to a negligible face specifity of the CO−Re adsorptive bond energy.

Regarding the rate of adsorption, we observe the typical precursor kinetics with an initially constant sticking coefficient near unity, indicating a very effective CO trapping and sticking, which has been described many times in the literature.[25]

Interesting is the relatively moderate work function increase of 780 meV produced by CO molecules on Re(10-10), compared to values reported for Ni(110), $\Delta\varphi_{max} > 1.3$ eV;[39] Ru(10-10), $\Delta\varphi_{max} = 1.15$ eV;[38] Co(10-10), $\Delta\varphi_{max} = 1.46$ eV[36] at 100 K; Pd(110), $\Delta\varphi_{max} = 1.085$ eV at 130 K.[43] For comparison, on the Re(0001) plane, a $\Delta\varphi_{max}$ of merely 555 meV is obtained,[12] also relatively small in comparison to CO on other TM surfaces with hexagonal symmetry, where often saturation values beyond 1 eV were reported. The reason may lie in specific orbital interactions between Re and CO, as discussed by Braun et al.[19] but also the overall reduced amount of adsorbable molecular CO due to the competing dissociation.

4.2. CO Dissociation and Atomic C + O Adsorption. Direct exposure to CO at 500 K exclusively feeds the dissociation channel and rapidly forms adsorbed C and O atoms. Accordingly, all observed features (LEED, TPD, and $\Delta\varphi$) reflect the interaction of these fragments with the Re surface. This holds in particular for the c(2 × 4) and p(1 × 2) LEED phases. Their sharpness, brightness, and low background intensity indicates a pronounced long-range order and an appreciable scattering factor of the involved adsorbates, whether a possible accompanying reconstruction of the Re surface contributes to the LEED intensity cannot be judged without a full dynamical structure analysis which is currently underway.[51] This would also address the question whether the observed c(2 × 4) phase stems from adsorbed O atoms *alone*, since in a former study of the oxygen interaction with the Re(10−10) surface, Lenz et al. just observed, among a sequence of other ordered O phases, a c(2 × 4) LEED pattern.[26]

Both phases apparently consist exclusively of CO dissociation products, viz., C and O atoms. These species likely form a random mixture (substitutional disorder) and not an ordered "surface alloy". In a previous investigation of CO dissociation on tungsten, this point was addressed by Wang and Gomer:[7] On W(100), 0.25 ML of adsorbed CO dissociate to form a c(2 × 2) LEED phase (total coverage $\Theta_{C+O} = 0.5$) with equal amounts of O and C atoms. However, for similar scattering factors, no decision between an ordered or substitutionally disordered coadsorbed phase could be made, although entropy arguments certainly favor the random distribution. By means of Tensor−LEED calculations, Döll et al.[52] have considered two-dimensional disordered alloys; by simply averaging over the individual scattering factors of the alloy constituents, they could even determine surface stoichiometries. Randomly mixed phases within adsorbed gas layers were recently reported in an STM study of the system NO/Ru(0001) by Nagl et al.[53] At sufficiently high temperatures, NO dissociates and forms a (2 × 2) phase which consists of a substitutionally disordered two-dimensional (N + O) mixed phase, representing a situation which is surprisingly similar to our (C + O)-on-Re case.

Another point concerns the driving force(s) to form these ordered phases. The c(2 × 4) phase with its nominal coverage $\Theta_{C+O} = 0.25$ allows a relatively open arrangement of the mutually interacting particles. Apparently, repulsive interaction forces operate in the [1-210] direction parallel to the troughs, while slight attractive forces act in the perpendicular [0001] direction leading to a centered structure. Thermal desorption measurements reveal that the c(2 × 4) phase still represents an

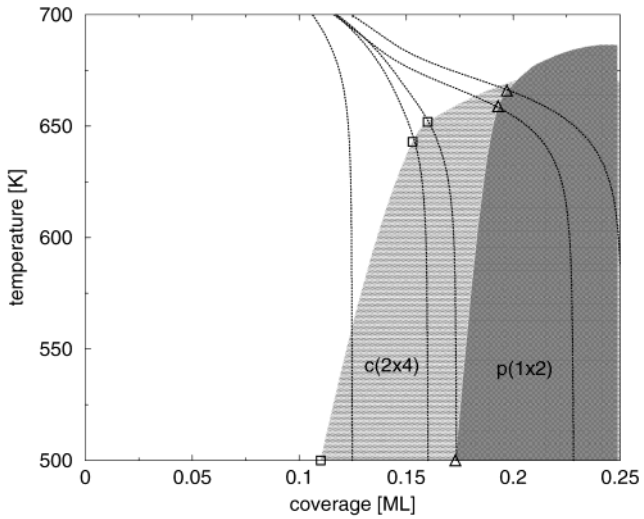

Figure 9. Schematic phase diagram of the c(2 × 4) and the p(1 × 2) mixed (C + O) phases in the $T-\Theta$ plane. The dotted (perpendicular) lines are $\Theta(T)$ curves taken from the TPD spectra of Figure 4. The triangles indicate the kinetic transitions from zero to second order (see text); the open squares mark the disappearance of the c(2 × 4) LEED intensities upon heating.

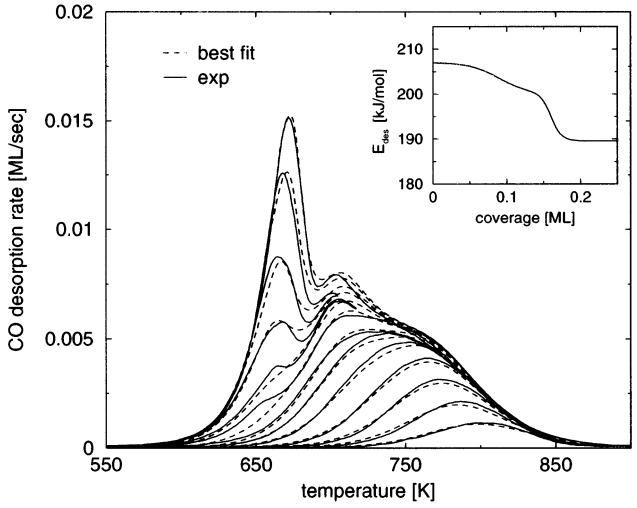

Figure 10. Series of experimental (full lines) and simulated TPD spectra (dashed lines) obtained by numerical integration of eq 1 and considering the change from zero to second order. See text for further details. The inset shows the coverage dependence of the heat of desorption as determined from the simulation.

energetically fairly favorable situation, with desorption energies of ~200 kJ/mol, cf. Figure 3. When the coverage approaches $\Theta_{C+O} = 0.5$, the empty spaces between the C (O) atoms in the [1-210] direction have become filled, and nearest-neighbor repulsions make the desorption energy of the fully developed (1 × 2) phase fairly sharply drop by ~10 kJ/mol to 189.5 kJ/mol. This is just a reasonable order of magnitude of this kind of mutual interaction energies.

In our *T*-dependent LEED measurements, we have observed, for both the c(2 × 4) and the p(1 × 2) phases, an order−disorder phase transition prior to C + O recombination and CO desorption, with critical temperatures around 650 and 670 K, respectively. The existence regime of the phases is schematically sketched in Figure 9. It is of some interest to assign the order of the respective phase transitions, i.e., whether these phases kind of *melt*, resulting in a lattice gas (or fluid) (first-order transition), or if they represent *continuous* transitions of the Landau type, with equal densities in the ordered and disordered phase. Landau's theory puts large restrictions on the symmetry of superstructures, which can exhibit the respective transitions: According to Schick,[54] there exist only three phases on a surface with 2-fold symmetry such as face-centered cubic (fcc) (110) or hcp (10-10), namely, p(1 × 2), p(2 × 1), and c(2 × 2), for which second-order phase transitions can occur. However, this argument cannot be reversed: Phase transitions observed with these phases are not necessarily of the second-order type, but could also be first-order. At any rate, we can state that the order−disorder transition of the c(2 × 4) structure must be of the first-order type, while that of the (1 × 2) could be both first or second order.

The quasi zero-order behavior of the desorption rate of the fully developed β_1 state may be considered as another manifestation of a phase equilibrium that prevails at fairly large coverages in the existence region of the p(1 × 2) phase. We assume that ordered islands of the (1 × 2) phase coexist with a dilute lattice gas of C + O atoms. The respective phase equilibrium provides a stationary concentration of 2D "gas phase" species and, hence, a Θ-independent rate of desorption, until the 2D condensed supply (p(1 × 2) islands) is exhausted. Similar effects have been found with Cu and Ag desorption from Re surfaces[55,56] and oxygen desorption from Au(110)[57] and were theoretically described by Kreuzer and Payne.[58] The 2D "gas phase" species may well be considered as transiently bound and mobile CO molecules (formed by successful recombination of $C_{ad} + O_{ad}$ as a transition state), which are about to leave the surface. Since the respective phase equilibrium involves the ordered p(1 × 2) phase, the dissolution of the respective phase can also be followed by LEED intensity measurements, the high-temperature limit of the coexistence region shows up as the disappearance of the (1 × 2) "extra" intensity.

To conclude our discussion on the energetics and kinetics of the Re(10-10)/CO system in the high-temperature region, we note that it is possible, by assuming appropriate functional dependences of both the pre-exponential factor ν and the desorption energy E_{des} in eq 1, to completely simulate the experimental TPD spectra of the recombining species C + O. For this purpose, we have integrated eq 1 for a given ν and E_{des} and evaluated E_{des} in each case by direct comparison with the experimental desorption rate. Figure 10 presents the obtained results: experimental data are drawn as full lines, calculated TPD spectra as broken lines. The theoretically determined coverage dependence $E_{des}(\Theta)$ is shown in the inset. Assumptions in this model are: (i) Apart from the zero-order behavior discussed above, the desorption obeys second-order kinetics; (ii) The pre-exponential factor is Θ independent but varies proportional to *T* (simple transition-state theory); (iii) E_{des} does not depend on *T* but only on coverage Θ. The agreement between the theoretical TPD spectra, determined by numerical integration of eq 1 under the use of the functions $\nu(T)$ and $E_{des}(\Theta)$, and the experimental data is actually very satisfactory, as Figure 10 demonstrates.

The peculiar dissociation activity of the Re(10-10) surface calls for a detailed comparison with the respective behavior of the basal Re(0001) orientation. In our work with CO/Re(0001),[12] we took CO TPD spectra under very similar conditions. A typical example is displayed in Figure 11 for comparison. The *molecular* CO states appear between 300 and 500 K and are the by far dominating species; the TPD state(s) between 700 and 850 K due to *dissociated* CO represent only a small fraction (less than 10%) of the overall amount of initially adsorbed gas. From experiments with stepped Re(0001) surfaces, Hously et

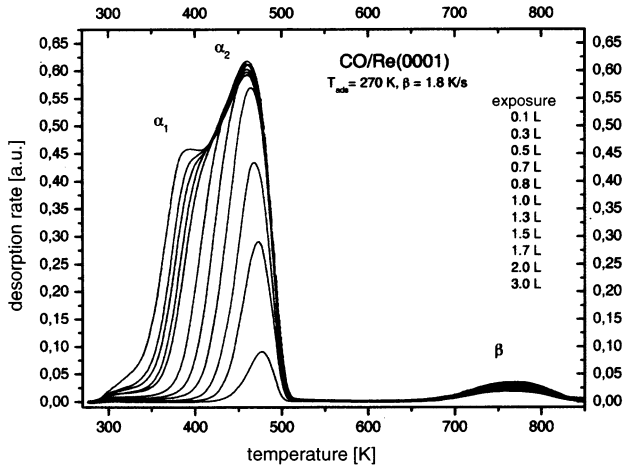

Figure 11. Series of thermal desorption spectra taken from CO/Re-(0001) after adsorption at 270 K with a heating rate of 1.8 K/s. Note the pronounced molecular α states and the quite weak (atomic) β states.[12]

al. deduced that CO dissociates preferentially at crystallographic defect sites.[13] By decorating and deactivating the respective (and, apparently, inevitably existing) defect sites with gold atoms, we could indeed show that the defect-free (0001) surface is no longer able to dissociate CO,[12] quite in contrast to the very active (10-10) surface of our present study. For this latter surface, the deposition of actually two gold monolayers is required to completely kill its CO dissociation activity.[59] Two major effects could be made responsible. A simple energetic view compares the energy gain (or effort) to cleave a C−O and a (CO)−Re bond and gain a C−Re and an O−Re bond instead. This argumentation is pursued (and calculated for the case of 3d and 4d transition metals) by Andreoni and Varma[9] but cannot explain mechanistic details of the dissociation reaction. Whether we invoke the highly coordinated CO adsorption sites of the "open" (10-10) surface as providing a particularly favorable local electronic configuration for filling CO's antibonding π^* orbitals or refer to the quantum chemical calculations by Hammer and Nørskov (who actually compared activation energies for CO dissociation on metals with different density of d electron states) the overall "chemical" result is the same: For the "borderline metals" with their peculiar d-band structure mentioned in the Introduction, one can establish a clear trend, whereafter less coordinated (high Miller-index) surfaces are active in dissociating CO, and this trend is entirely confirmed in our study dealing with Re(10-10) and Re(0001). The CO interaction with the (flat) (110)[8] and the less densely packed W(100) surface[6,7] has already been mentioned to exhibit remarkable differences in their CO dissociation activity. Another "borderline" metal, cobalt, needs an even more pronounced crystallographic corrugation for becoming dissociation-active: While the Co(0001) and the Co-(10-10) surfaces do not spontaneously dissociate CO,[35,36] the still rougher Co(11-20) face is active in cleaving the C−O bond.[37] The same thing holds, by the way, for ruthenium, where the "lower"-index planes (0001) and (10-10) do not dissociate CO but the "higher-index" plane (11-21) readily does.[60]

Acknowledgment. The authors gratefully acknowledge financial support by Deutsche Forschungsgemeinschaft (SFB 290).

References and Notes

(1) Ford, R. R. *Adv. Catalysis* **1970**, *21*, 51.
(2) Rogozik, J.; Dose, V. *Surf. Sci.* **1986**, *176*, L847.
(3) Campuzano, J. C. In *The Chemical Physics of Solid Surfaces and Heterogeneous Catalysis*; King, D. A., Woodruff, D. P., Eds.; Elsevier: Amsterdam, 1990; Vol. 3A, Chapter 4, p 389.
(4) Hammer, B.; Morikawa, Y.; Nørskov, J. K. *Phys. Rev. Lett*. **1996**, *76*, 2141.
(5) Brodén, G.; Rhodin, T. N.; Brucker, C.; Benbow, R.; Hurych, Z. *Surf. Sci*. **1976**, *59*, 593.
(6) Anderson, J.; Estrup, P. J. *J. Chem. Phys*. **1967**, *46*, 563 [CO on W(100)].
(7) Wang, C.; Gomer, R. *Surf. Sci*. **1979**, *90*, 10 [CO on W(100)].
(8) (a) Kohrt, C.; Gomer, R. *Surf. Sci*. **1971**, *24*, 77. (b) Kohrt, C.; Gomer, R. *Surf. Sci*. **1973**, *40*, 71 [CO on W(110).
(9) Andreoni, W.; Varma, C. M. *Phys. Rev*. **1981**, *B 23*, 437.
(10) (a) Blyholder, G. *J. Phys. Chem*. **1964**, *68*, 2772. (b) Blyholder, G. *J. Phys. Chem*. **1975**, *79*, 756.
(11) Mavrikakis, M.; Hammer, B.; Nørskov, J. K. *Phys. Rev. Lett*. **1998**, *81*, 2819.
(12) Weingart, A.; Christmann, K., to be published.
(13) Housley, M.; Ducros, R.; Piquard, G.; Cassuto, A. *Surf. Sci*. **1977**, *68*, 277.
(14) Ducros, R.; Alnot, M.; Ehrhardt, J. J.; Hously, M.; Piquard, G.; Cassuto, A. *Surf. Sci*. **1980**, *94*, 154.
(15) Ducros, R.; Housley, M.; Piquard, G.; Alnot, M. *Surf. Sci*. **1981**, *109*, 235.
(16) Ducros, R.; Tardy, B.; Bertolini, J. C. *Surf. Sci*. **1983**, *128*, L219.
(17) Tatarenko, S.; Alnot, M.; Ehrhardt, J. J.; Ducros, R. *Surf. Sci*. **1985**, *152/153*, 471.
(18) Braun, W.; Meyer-Ehmsen, G.; Neumann, M.; Schwarz, E. *Solid State Commun*. **1979**, *30*, 605.
(19) Braun, W.; Meyer-Ehmsen, G.; Neumann, M.; Schwarz, E. *Surf. Sci*. **1979**, *89*, 354.
(20) He, J. W.; Goodman, D. W. *J. Phys. Chem*. **1990**, *94*, 1502.
(21) Zehner, D. M.; Farnsworth, H. E. *Surf. Sci*. **1972**, *30*, 335.
(22) Kelly, D. G.; Gellman, A. J.; Salmeron, M.; Somorjai, G. A.; Maurice, V.; Huber, M.; Oudar, J. *Surf. Sci*. **1988**, *204*, 1.
(23) Clavenna, L. R.; Schmidt, L. D. *Surf. Sci*. **1972**, *33*, 11.
(24) Menzel, D. In *Interactions on Metal Surfaces, Springer Series Topics in Applied Physics*; Gomer, R., Ed.; Springer: Berlin, Heidelberg, New York, 1975; Vol. 4, p 101.
(25) Morris, M. A.; Bowker, M.; King, D. A. In *Chemical Kinetics - "Simple Processes at the Gas − Solid Interface"*; Bamford, C. H., Tipper, C. F. H., Compton, R. G., Eds.; Elsevier: Amsterdam, 1984; Chapter I, Vol. 19, and references given therein.
(26) Lenz, J.; Rech, P.; Christmann, K.; Neuber, M.; Zubrägel, C.; Schwarz, E. *Surf. Sci*. **1992**, *269/270*, 410.
(27) Parschau, M.; Christmann, K. *Surf. Sci*. **1996**, *347*, 63.
(28) Döll, R.; Hammer, L.; Heinz, K.; Bedürftig, K.; Muschiol, U.; Christmann, K.; Seitsonen, A. P.; Bludau, H.; Over, H. *J. Chem. Phys*. **1998**, *108*, 8671.
(29) Pauls, C. Ph.D. Thesis, FU Berlin, and in preparation
(30) Christmann, K.; Muschiol, U. *Z. Phys. Chem*. **1996**, *197*, 155.
(31) Redhead, P. A. *Vacuum* **1962**, *12*, 203.
(32) Wagner, R.; Christmann, K. *Surf. Sci*. **2000**, *469*, 55.
(33) Habenschaden, E.; Küppers, J. *Surf. Sci*. **1984**, *138*, L147.
(34) King, D. A.; Wells, M. G. *Proc. R. Soc*. **1974**, *A339*, 245.
(35) Bridge, M. E.; Comrie, C. M.; Lambert, R. M. *Surf. Sci*. **1977**, *67*, 393 [CO on Co(0001)].
(36) Papp, H. *Ber. Bunsen−Ges. Phys. Chem*. **1982**, *86*, 555 [CO on Co(10-10)].
(37) Prior, K. A.; Schwaha, K.; Lambert, R. M. *Surf. Sci*. **1978**, *77*, 193 [CO on Co(11-20)].
(38) Lauth, G.; Solomun, T.; Hirschwald, W.; Christmann, K. *Surf. Sci*. **1989**, *210*, 201.
(39) Madden, H. H.; Küppers, J.; Ertl, G. *J. Chem. Phys*. **1973**, *58*, 3401 [CO on Ni(110)].
(40) Madden, H. H.; Ertl, G. *Surf. Sci*. **1973**, *35*, 211 [CO on Ni(110)].
(41) Bowker, M.; Guo, Q.; Joyner, R. *Surf. Sci*. **1991**, *253*, 33 [CO on Rh(110)].
(42) Ertl, G.; Rau, P. *Surf. Sci*. **1969**, *15*, 443 [CO + on Pd(110)].
(43) He, J. W.; Norton, P. R. *J. Chem. Phys*. **1988**, *89*, 1170 [CO on Pd(110)].
(44) Hofmann, P.; Bare, S. R.; King, D. A. *Surf. Sci*. **1982**, *117*, 245 [CO on Pt(110)].
(45) Christmann, K.; Ertl, G. *Z. Naturforsch*. **1973**, *A28*, 1144 [CO on Ir(110)].
(46) Lambert, R. M. *Surf. Sci*. **1975**, *49*, 325.
(47) Palmberg, P. W.; Tracy, J. C. *J. Chem. Phys*. **1969**, *51*, 4852.
(48) Ertl, G. In *The Nature of the Surface Chemical Bond*; Rhodin, T. N., Ertl, G., Eds.; North-Holland: Amsterdam, 1979; p 364.
(49) Conrad, H.; Ertl, G.; Koch, J.; Latta, E. E. *Surf. Sci*. **1974**, *43*, 462.
(50) Helms, C. R.; Madix, R. J. *Surf. Sci*. **1975**, *52*, 677.

(51) Pauls, C.; Schwede, S.; Kickbusch, R.; Christmann, K. *Verhandl. DPG*, to be published.
(52) Döll, R.; Kottke, M.; Heinz, K. *Phys. Rev.* **1993**, *B48*, 1973.
(53) Nagl, C.; Schuster, R.; Renisch, S.; Ertl, G. *Phys. Rev. Lett.* **1998**, *81*, 3483.
(54) Schick, M. *Prog. Surf. Sci.* **1981**, *11*, 245.
(55) Wagner, R.; Schlatterbeck, D.; Christmann, K. *Surf. Sci.* **1999**, *440*, 231.
(56) Wagner, R. Ph.D. Thesis, Free University, Berlin, 2003.
(57) Gottfried, M. Ph.D. Thesis, Free University, Berlin, 2003.
(58) Kreuzer, H. J.; Payne, S. H. In *Dynamics of Gas−Surface Reactions*; Rettner, C. T., Ashfold, M. N. R., Eds.; Cambridge: 1991; p 220.
(59) Pauls, C.; Christmann, K., in preparation.
(60) Fan, C. Y.; Bonzel, H. P.; Jacobi, K. *J. Chem. Phys.* **2003**, *118*, 9773.